

Astro2020 APC White Paper

A Beam-Forming Receiver for the GBT at 23 GHz

Type of Activity: Ground Based Project Space Based Project
 Infrastructure Activity Technological Development Activity
 State of the Profession Consideration Other

Principal Author:

Name: Larry Morgan
Institution: Green Bank Observatory
Email: lmorgan@nrao.edu
Phone: (304) 456-2399

Co-authors: Will Armentrout, David Frayer, Laura Jensen, Felix J Lockman, Karen O’Neil, Steve White (GBO)
Loren Anderson (WVU)
Esteban D. Araya (WIU)
Kevin Bandura (WVU)
Sara Cazzoli (IAA-CSIC)
James Di Francesco (NRC)
Erik Rosolowsky (U.Alberta)
Sarah Sadavoy (SAO)
Martin Sahlén (Uppsala University)
John Tobin (NRAO)

Project Endorsers: Hèctor Arce (Yale University), Tracy Becker (Southwest Research Institute), Robert Benjamin (UWW), Anamaria Berea (Ronin Institute), Sriram Bhiravarasu (Lunar and Planetary Institute), Amber Bonsall (GBO), Natalie Butterfield(GBO), Suchetana Chatterjee (Presidency University), Claudia Cicone (INAF, University of Oslo), Filippo D’Ammando (INAF-IRA Bologna), Chuanfei Dong (Princeton University), Olivier Doré (JPL/Caltech), Rachel Friesen (NRAO), Frank Ghigo (GBO), Tapasi Ghosh (GBO), J. Colin Hill (Institute for Advanced Study), Taylor Hogge (BU), Amanda Kepley (NRAO), Natalia Lewandowska (WVU), Ryan Lynch (GBO), Ron Maddalena (GBO), Brett McGuire (NRAO), Toney Minter (GBO), Eric Perlman (Florida Institute of Technology), Dominic Pesce (CfA), Francesco Piacentini (Dipartimento di Fisica, Sapienza University of Rome), Daryl Reynolds (WVU), Graca Rocha (JPL/CalTech), Chris Salter (GBO), Natalia Schmid (WVU), Andrew Seymour (GBO), David Thilker (Johns Hopkins University), Francisco Villaescusa-Navarro (Center for Computational Astrophysics, Flatiron Institute), Karl Warnick (BYU), Brian Woerner (WVU), Jun-Hui Zhao (CfA)

Executive Summary:

We propose to support the design, construction and commissioning of a K-band (18-26 GHz) 256 element phased array feed (PAF) receiver and associated beam-former capable of forming 225 independent beams (i.e. a 225 pixel spectroscopic camera), for the 100m diameter Green Bank Telescope (GBT). This instrument will vastly improve the mapping speed at K-band in comparison to the existing GBT seven pixel receiver, currently in use, which is the third most sought-after receiver on the GBT, in terms of requested hours.

The proposed receiver will simultaneously observe the (1,1), (2,2), and (3,3) inversion transitions of ammonia, a critically important probe of dense molecular gas that can trace kinetic temperatures, optical depth and column densities simultaneously with minimal bias. There are other molecular tracers of star formation activity observable at this frequency band, including CCS and HC₇N, which act as ‘chemical clocks’ and thus can distinguish between different modes of star formation (e.g. Seo et al., 2019). Water masers are also strong emitters in the range of the proposed receiver, tracing shocked gas and outflow motions in low- and high-mass star-forming regions (see Walsh et al., 2011) in addition to providing distance measurements to nearby active galaxies, yielding a direct measurement of the Hubble constant, independent of standard candles (Braatz et al., 2019). Furthermore, several radio recombination lines, including hydrogen and carbon transitions between 63 α and 70 α , will be observable, which will allow comprehensive studies of ionized gas and photon-dominated regions in star-forming regions and planetary nebulae.

The GBT presents a 100m unblocked active surface, providing a combination of higher gain, higher sensitivity and better angular resolution at K-band than any other radio telescope. In comparison, interferometers such as the Very Large Array (VLA) offer higher angular resolution but simply do not have the sensitivity to large scales needed to detect extended emission from dense clumps within molecular clouds. The $\sim 32''$ angular resolution of the GBT at 23.7 GHz is well-matched to star-forming substructures in nearby clouds (0.07 pc at 450 pc, the distance of Orion) and the field-of-view of the instrument will surpass that of the 2' primary beam of the VLA, providing excellent short-spacing data for combination with interferometric observations.

Construction will be a collaboration between the West Virginia University (WVU) Lane Department of Computer Science and Electrical Engineering, the WVU Department of Physics and Astronomy, and the Green Bank Observatory (GBO). These groups have an outstanding track record of developing, building and using similar instrumentation at the GBT and elsewhere.

Development of the proposed PAF will involve both undergraduate and graduate students in engineering and scientific research activities. Undergraduate students will assist with the design and validation of the instrument as part of their engineering senior design projects. Graduate students will participate as research assistants, heavily involved in testing and commissioning the instrument. The GBT is one of the very few remaining world class radio telescopes where students can obtain hands-on experience in instrument development. This is a critical aspect of training the next generation of instrumentalists.

1 Key Science Goals and Objectives

Understanding the process of star formation is one of the major efforts in modern astrophysics¹, as star formation impacts a broad range of topics, from the formation of planets to the cosmic evolution of galaxies. This has, to-date, been largely an endeavor confined to the Milky Way, although the advent of the high-resolution offered by the VLA, ALMA and the forthcoming ngVLA now allow for significant extragalactic studies of the molecular clouds home to the ‘cores’ and ‘clumps’ from which young stars form (see PHANGS-ALMA², Leroy et al. 2019, 2018a,b,c, 2017).

Star formation is studied with the assistance of catalogues of thousands of sources, which have observational data ranging across the entire electromagnetic spectrum. Although there is considerable breadth in the wavelength range represented by these surveys³, there is a focus on the infrared and submillimeter portions of the spectrum due to the low opacity of the material traced at these wavelengths. These dense regions with high star-forming rates show significant substructure on scales from the 100 pc molecular cloud size, through parsecs-long filaments which permeate the clouds, to cores, which in a bound state form the primordial unit of star formation, the Young Stellar Object (YSO).

Beyond identifying a qualitative outline of the hierarchical structure found in and around star-forming regions, we wish to establish a more definitive physical description of the star-forming process. Such a description would incorporate, for example, the level of thermal, turbulent and magnetic support for small-scale clouds. On the larger scale of filaments, some key questions are raised by Friesen et al. in their Astro2020 white paper (Friesen, 2019), i.e. [i] How does gas in clouds assemble into filaments and cores? [ii] How will the gas in these substructures evolve? [iii] Is there further coherent substructure within filaments (e.g. “fibers”; Hacar et al. 2017, 2013); [iv] What fraction of starless cores are transient and what fraction form stars?

Furthermore, and increasing the scale still further, Leroy et al. ask in their Astro2020 white paper (Leroy et al., 2019) [i] How do the distributions of density, turbulence, temperature, and dynamical state in the cold ISM depend on [...] local environment? [ii] How do these physical conditions regulate the rate at which stars form from cold gas and the properties of the newborn stars and clusters? [iii] How do these physical conditions reflect and regulate the impact of stellar feedback?

These questions may all be answered through the systematic observations of the dense gas present in cores and filaments. While there are several molecular tracers which can accomplish this to varying degrees, ammonia (NH_3) is one of the most commonly used, due to its properties which provide measurements of gas kinetic temperature, excitation temperature, opacity and hence column density. The occurrence of the ($J=1, K=1$) and ($J=2, K=2$) lines of ammonia, along with their hyperfine components, within a single 200 MHz window around 23.7 GHz (radio astronomy’s K-band) means that these physical properties are being directly measured through

¹‘Star and Planet Formation’ and ‘Galaxy Evolution’ are the two, approximately equal, leading topics in proposals explicitly requesting GBT observations in Astro2020 white papers (<https://greenbankobservatory.org/science/astro2020/>)

²<https://public.nrao.edu/news/2019-alma-phangs/>

³see the RMS, *MSX*, *GLIMPSE*, *WISE*, 2MASS, ATLASGAL, MOXC2, CORNISH, GLOSTAR, *MIPSGAL*, *HiGAL*, BGPS, SEDIGISM, MAGPIS and THOR surveys

the same optical path and originate at the same scale in the observed gas. This removes many sources of measurement error and bias that affect measurements of these properties obtained through observations of other molecules (e.g. CO and its isotopologues).

A K-band receiver with seven pixels (the K-band Focal Plane Array, KFPA) is currently operational on the GBT and provides unique capabilities worldwide. It was commissioned in 2009-2010 and has been used in observations across multiple fields of astronomy, though it has performed particularly well for large scale mapping projects. It was the third most requested receiver on the GBT over the last two semesters (based on hours requested) and is currently serving as the primary instrument for three separate large-scale surveys focussing on different aspects of star formation, the Green Bank Ammonia Survey (GAS; Friesen et al. 2017) which aims to observe all northern Gould Belt star-forming regions with $A_V > 7$; the K-band Examinations of Young Stellar Object Natal Environments (KEYSTONE; Keown et al., *in prep*) survey and the Radio Ammonia Mid-Plane Survey (RAMPS; Hogge et al. 2018) which has recently completed its pilot phase with a low sensitivity, wide-field survey of the Galactic plane. Each of these surveys used 300-500 hours on the GBT, which at the time had an available amount of 6,000 hours a year for open skies projects across the whole frequency range of 0.29 - 116 GHz. The large fraction of time given to these projects, all within the same observing band, illustrates the community's desire for ammonia observations as well as the strong science case backing these up. However, the limited mapping speed of the KFPA has enabled the study of only the very highest column density locations. The resulting bias may make the results of these large surveys much less general than if a broader range of column densities were sampled. Tantalizingly, early GAS analysis has revealed the presence of low- brightness NH_3 emission at locations of $A_V < 7$, offering the prospect of probing the flow of gas directly into star-forming cores and filaments if such emission were detected more robustly (Friesen, 2019).

We illustrate the power, and also the limitations, of the KFPA in Fig. 1. Here, we show *Herschel* dust emission and GBT NH_3 observations of Orion A in the left-most panel. The NH_3 map probes the densest parts of the filaments and contains a wealth of information on the physical state of the gas. However, this figure also clearly indicates that the full extent of the material visible in the *Herschel* observations is not traced by the NH_3 maps. Derivation of the kinetic temperature shown in the right-most panel requires detection of the NH_3 (2,2) line; the regions of the map with poor signal in this transition leads to the patchiness of the derived values. Without accurate kinetic temperatures we cannot determine the turbulent contributions to the line widths, and hence accurately measure the dynamical states of the dense gas substructures. The KFPA is theoretically capable of reaching the sensitivities required to fully complement the *Herschel* submillimeter data. However, covering the large regions of the sky necessary to make this scientifically worthwhile would be prohibitively time-consuming with the KFPA.

It is worth reiterating the low errors and bias of the kinetic temperature and opacity measurements derived from NH_3 observations. While the dust temperature of star-forming material may be derived from the multi-wavelength *Herschel* SPIRE/PACS maps, this measurement is prone to large errors (e.g. from the dust opacity assumed for the region in question). In addition to providing unambiguous kinetic temperature measurements, NH_3 observations also provide kinematic information, unobtainable from submillimeter observations of interstellar dust. In order to understand the evolution and development of star-forming structures from molecular clouds to filaments and down to the scale of individual cores, it is essential to trace these kinematics.

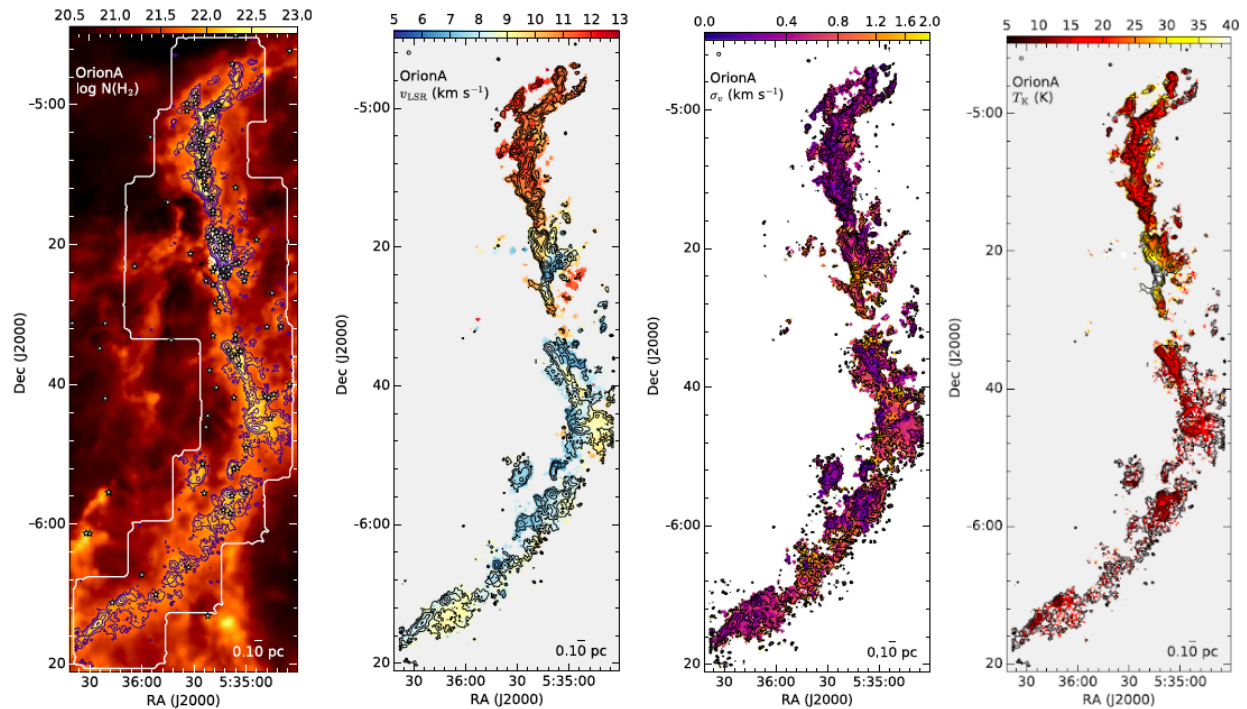


Figure 1: NH_3 properties of Orion A from GAS (Friesen et al., 2017). The left panel shows *Herschel*-derived column density data, inferred from dust emission, with NH_3 integrated intensity overlaid and Spitzer protostars shown. The next panel shows the LSR velocity, exhibiting a clear north-south gradient. The third panel shows the velocity dispersion and the fourth shows the kinetic temperature derived from the (1,1) and (2,2) line ratios.

While the KFPA has been an effective and productive instrument, it was always intended as a pathfinder for a larger descendant, originally expected to be of a similar design but with, perhaps, 64 feeds. In recent years, however, significant progress has been made on an alternate technology that promises to deliver multi-pixel capabilities more efficiently, and with better characteristics than traditional feed-horn based receivers. A phased array feed receiver uses many small receiving elements whose output is then cross-correlated, forming independent beams (pixels) on the sky. Unlike feed-horn technology, in which the spacing of the pixels is rather sparse because of the physical size of the horns, the pixels of a PAF receiver can be placed in an arbitrarily tight pattern, leading to higher observing efficiency, making deep surveys of large areas of the sky possible.

The GAS project has shown that a sensitivity limit of $\sim 0.1 \text{ K rms}$ in 0.1 km s^{-1} channels is required to detect NH_3 at locations with $A_V \sim 7$. Using the KFPA, a one square-degree map at this sensitivity requires 50 telescope hours, excluding overheads. At this rate, it would take ~ 8000 hours to map the 160 square-degrees covered by the *Herschel* Gould Belt Survey (GBS). This would take several years, even if the GBT were devoted solely to such a project. It is estimated that the proposed receiver could accomplish this in only ~ 800 hours, which when spread out over multiple semesters would be quite feasible. Note that the single-polarisation nature of the PAF feeds and a slightly higher T_{sys} leads to an improvement in mapping speed of a factor of ten, while the increase in the number of beams on the sky might initially suggest a greater factor.

Wide-field surveys would also benefit significantly from more efficient observations. Due to the large amount of time required and the pressure of oversubscription at certain LST ranges, surveys, such as RAMPS, typically avoid the Galactic center. This is especially unfortunate given the large amount of dense gas and interesting physics in the region. A K-band PAF would enable a complete census of dense clouds across the entire inner Galaxy at the critical sensitivity limit associated with $A_V \simeq 7$.

In addition to the potential of a K-band PAF as a survey instrument for Galactic molecular clouds, there are other scientific applications that would benefit from such an instrument. There have been at least eight Astro2020 white papers submitted in the ‘Thematic Areas’ of Galaxy Evolution (Butterfield et al., 2019; Leroy et al., 2019), Star and Planet Formation (Friesen, 2019; McGuire, 2019a,b; Remijan, 2019), Planetary Systems (Margot et al., 2019), and Resolved Stellar Populations and their Environments (Thilker et al., 2019) which all specifically state the need for either a large heterodyne array at K-band on the GBT or for science which would explicitly benefit from the same. There are significantly more decadal survey papers which request a similar instrument in less explicit terms, either at an unspecified frequency band, as a short-spacing addition to VLA or ngVLA observations or as a pathfinder to new science and/or technology.

Furthermore, there is great potential for a heterodyne array which can instantaneously sample a full field-of-view of $\sim 8'$ on the GBT, particularly when used as a short-spacing instrument in conjunction with the VLA or ngVLA, which have primary beam sizes at K-band of $2'$ and $3'$, respectively. There were at least seven publications in 2018 which used the current KPAF for just this purpose, either as part of the VLBI program or for other short-spacing observations (Bietenholz et al., 2018; Kutkin et al., 2018; Monsch et al., 2018; Pilipenko et al., 2018; Sokolov et al., 2018; Williams et al., 2018; Zhao et al., 2018).

2 Technical Overview

2.1 Overall Architecture and System Specifications

A block diagram of the proposed PAF is shown in Fig. 2. It is comprised of a focal plane array of 256 horn antennas followed by cryogenic LNAs cooled to 15 K. The signals are then mixed down and bandpass filtered to an IF of 400-800 MHz. The signals then transition to an RF over fiber (RFOF) system to carry the data over 128 individual fibers to the shielded control room in the Jansky Laboratory, approximately one mile from the telescope. Here the signals have a final bandpass and analog amplification stage before being digitized by the ICE System (Bandura et al., 2016). The ICE System plus GPU node farm perform the real-time correlation and beam-forming. The final data products are then stored on the existing Green Bank Lustre high speed data storage system.

2.2 Performance Specifications

The KPAF design specifications are summarized in Table 1.

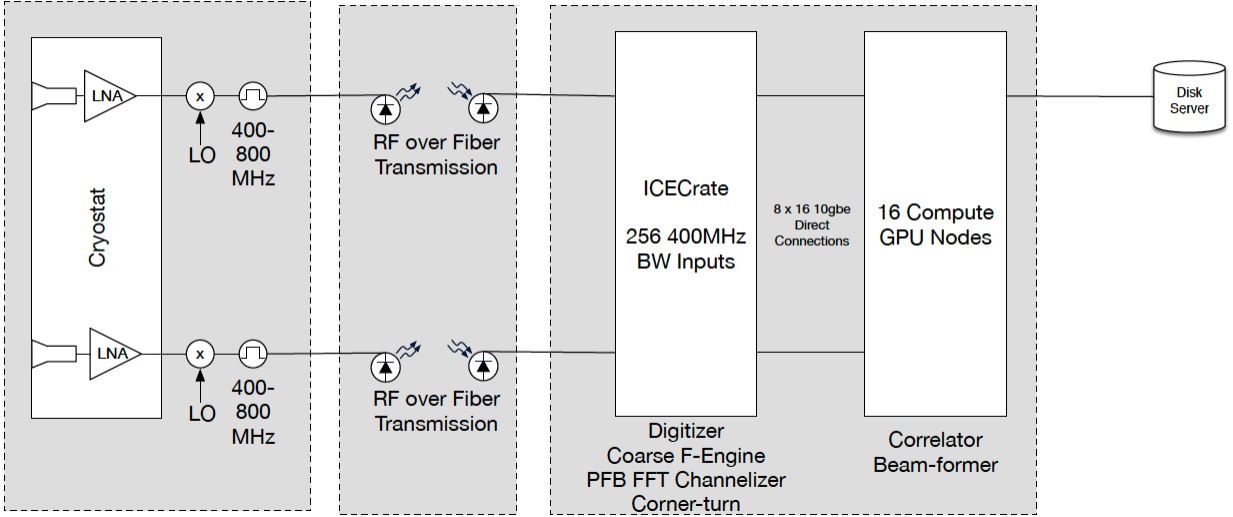


Figure 2: Block diagram of the proposed PAF system.

Table 1: Performance Specifications.

Number of Feed-horns	256
Number of Beams	225
Instantaneous Bandwidth	400 MHz
Tunable Frequency Range	18 - 26 GHz
Fine Frequency Resolution	30 kHz
System Temperature	50 K
Sky Sensitivity (T_{sys}/η_{beam})	< 85 K

2.3 The Phased Array Feed

The feeds for phased array receivers are constrained in size so that the feed spacing allows for Nyquist-sampling of the fields in the focal plane. Yet in order to form the maximum number of beams to satisfy the mapping speed criteria, the size of the feed array must be large enough to efficiently sample many of the Airy patterns formed by the main surface in the focal plane. For the K-band frequency range, a pyramidal feed-horn meets these criteria. These can be machined from aluminum using relatively standard procedures.

2.3.1 Pyramidal Feed-Horn

The Nyquist sampling criteria is $\lambda \frac{f}{D}$, thus the dimension of the feed-horn aperture must be less than this at a nominal wavelength. For the frequency coverage of the proposed PAF, the nominal wavelength, λ_0 , will be taken at mid-band of the range 22.24 - 25.43 GHz, or 1.28 cm. Full electromagnetic simulations of the E and H-plane beam patterns of such a horn are shown in Fig. 3.

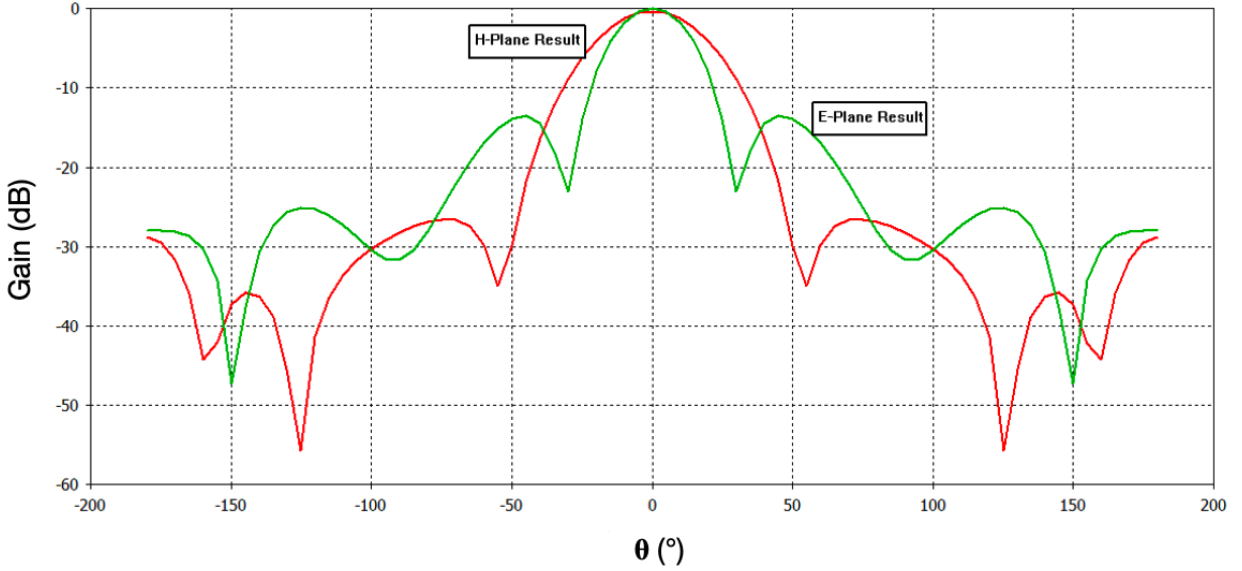


Figure 3: Simulated farfield beam patterns at 23.4 GHz for a pyramidal horn, showing the electric field plane (E-plane) in green and the magnetic field plane (H-plane) in red.

2.3.2 PAF Efficiency

With coverage of the Airy pattern from four horns, the beam-formed efficiency is estimated to be 0.61. For an array of 16×16 elements which encompasses one half-meter diameter, the maximum number of independent beams which can be formed is $15 \times 15 = 225$. With an estimated system temperature of $T_{\text{sys}} = 50$ K, we can estimate a mapping speed parameter⁴ through:

$$N \left(\frac{\eta_{\text{PAF}}}{T_{\text{sys}}} \right)^2 = 225 \left(\frac{0.61}{50} \right)^2 = 0.0335 \text{ K}^{-2} \quad (1)$$

In contrast, the current dual-polarization seven-beam K band focal plane array achieves 0.0035 K^{-2} , with seven horns, 40 K T_{sys} , and 0.63 efficiency. The improvement is a factor of approximately 10, and may be improved upon if more feeds are included in the beam-forming at the center of the array.

2.4 Remaining PAF Components

The entire system will be cryogenically cooled, with a dewar designed by the experienced team at GBO. The low noise amplifier will be built with a commercial MMIC device taking advantage of economies of scale, reduced size and ease of use. The Custom Microwave CMD160 covers the desired frequency range, has reasonable gain and return loss, and relatively low power consumption. A conservatively estimated noise temperature of 13 K is competitive with the

⁴This equation is based upon the proportionality of the time taken to reach a given rms level (σ) to the inverse square of that rms, i.e. $t \propto \frac{1}{\sigma^2}$ and the radiometer equation, which gives $t \propto \left(\frac{\eta}{T_{\text{sys}}} \right)^2$

current Central Development Laboratory cryo3 devices (8 K), which have a much larger mechanical footprint and a complex biasing scheme. Since this PAF will be single polarization, the amplifiers interface directly to the cooled feed array. Thus, the receiver temperature is conservatively expected to be equal to that of the KFPA receiver.

An integrated down converter module accepts the microwave frequencies, converts the band to an intermediate frequency, filters the input to the band limited 400 MHz, then down converts to the frequency range of the optical modulators. This design will be leveraged from the previous KFPA integrated downconverter modules design with only slight modifications required.

2.5 The IF Section and Fiber Transmission

The transmission of signals from the GBT receiver cabin to the equipment room in the Jansky Laboratory will be done using RFOF links. The links are based around a Fabry-Perot laser over a single mode fiber. Such a system has been prototyped for the CHIME telescope (Mena et al., 2013). The proposed version will utilize a bandwidth from 400-800 MHz. A roughly zero-gain system directly feeding the laser has a noise figure of 27 dB. This can be vastly reduced using an amplifier on the input. Gain can be easily added to the output to adjust the overall signal level into the beam-former.

To reduce the total number of fibers required, two IF signals will be duplexed onto each fiber. The signals will be mixed down to two different IF ranges of 400-800 MHz and 1.6-2 GHz, and then duplexed onto a single fiber. At the receiving side of the fiber, these can then be mixed with a single LO separating out the upper-sideband and lower-sideband. This means that only 128 fibers total will be required, easily within the remaining capacity which exists in the 288-fiber bundle already installed between the GBT and the Jansky Laboratory.

2.6 The Beam-Former

The correlator will be based on an ICE-system design (Bandura et al., 2016). The overall system architecture is comprised of sixteen ICE-motherboards in an ICE-crate with a full-mesh backplane. Each motherboard has ADC daughter-boards, processing 16 analog inputs each for a total of 256 inputs. The system is designed to flexibly scale up to 2048 inputs without requiring additional networking hardware. The digitizers are based around EV8AQ160 ADCs, where each ADC chip can sample 4 inputs at 8 bits at 1.25 GSPS. This system would operate them at 800 MSPS and sample the IF in the second Nyquist zone from 400-800 MHz. The ADCs are able to provide a spur-free dynamic range of 52 dBc, and 7.5 effective bits. The system is scalable to have increased bandwidth at the sacrifice of inputs.

Two daughter-boards are connected to each ICE motherboard (see Fig. 4). Each ICE motherboard processes the input from 16 analog inputs. The digitized signal is then channelized into 1024 frequencies using a poly-phase filter bank FFT from the CASPER library. The data width is then reduced to 4 bit + 4 bit complex values per frequency channel. The frequencies selected here can be set to process the entire 400 MHz, or send out multiple copies of the same frequencies. This allows for multiple compute nodes to process the same frequency subset.

The data are then processed through the ICE-system custom-backplane corner-turn network

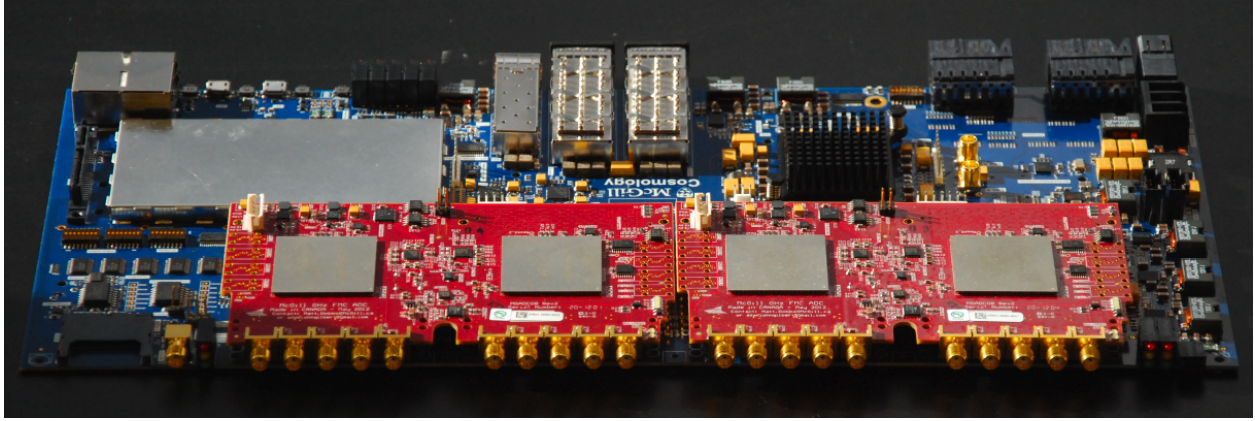


Figure 4: ICE motherboard shown with two FCM daughterboards. Each input sampled with 8 bits at up to 1.25 GSPS.

(Bandura et al., 2016), such that each motherboard has the information from 256 inputs for 64 frequency channels. The data are then packetized into standard Ethernet UDP packets to be sent via a direct link to a set of 16 high-performance computing nodes, at a data rate of ~ 7.3 Gbps per link, for a total of ~ 900 Gbps total data rate.

The compute nodes are then responsible for further channelization, correlation, beam-forming, and time averaging. Each node operates independently, processing its own subset of frequencies received from the ICE-crate. Each node receives data on eight 10 GbE links utilizing a pair of network interface cards which each are in turn connected via $8 \times$ PCI version 3 to the node. The nodes themselves are diskless and are controlled from an additional node which serves the OS, software, and a data buffer for the nodes. Each node hosts two AMD GPUs which perform the bulk of the computation.

The GPUs are utilized for the computation of the full correlation matrix and integration in time of the output matrix. The GPUs can also perform further channelization of the spectrum. The coarse channelization does affect the final output channelization, particularly at the coarse channel edges. Care must be taken to ensure full sensitivity at higher frequency resolutions.

Calculating the full correlation matrix allows the beam-former to be completely flexible in calibrating the full system and forming any possible beams on the sky. This is different from the traditional weighted-sum beam-former. This comes at a significant computational cost compared to the possible FFT beam-forming using a regular input array (N^2 vs $N \log N$). However, the power and flexibility will prove invaluable for creating a stable instrument.

3 Cost and Scheduling

The proposed design includes both the front-end and the back-end of the instrument. The front-end includes dewar design and construction, horn antennas, filtering, ultra-low-noise amplification, and RFOF communications to the Green Bank control room. The back-end includes high-speed digital-to-analog conversion, correlation, and beam-forming using a GPU node farm and our PI-developed ICE boards, which are custom designed as a low-cost scalable

telescope signal processing system. A full description of project funding is still being developed, as such we are simply providing the categorisation for the overall project as 'small' as defined by the NAS⁵, this includes all science and operations activities. The main activities and projected timeline for the project are shown in Fig. 5

WVU and GBO staff have successfully collaborated on several cryogenic receiver projects (the KFPA, a feed-horn array, the FLAG L-band (1.4 GHz) phased array feed (PAF) and the CHIME (Bandura, K., et al., 2014) correlator/beam-former). WVU and GBO personnel have also supported interfacing and commissioning the FLAG beam-former on the GBT. In addition, a collaborative proposal submitted to the NSF's Major Research Instrumentation program by Brigham Young University and WVU (P.I. K.Warnick) includes some budget for a simple prototype K-band PAF. This is based on work several years ago with a 70-90 GHz PAF. Calibration is not easy at frequencies well above L band ~ 1 GHz, so this K band PAF is intended to serve to build expertise with respect to calibration and other technical issues.

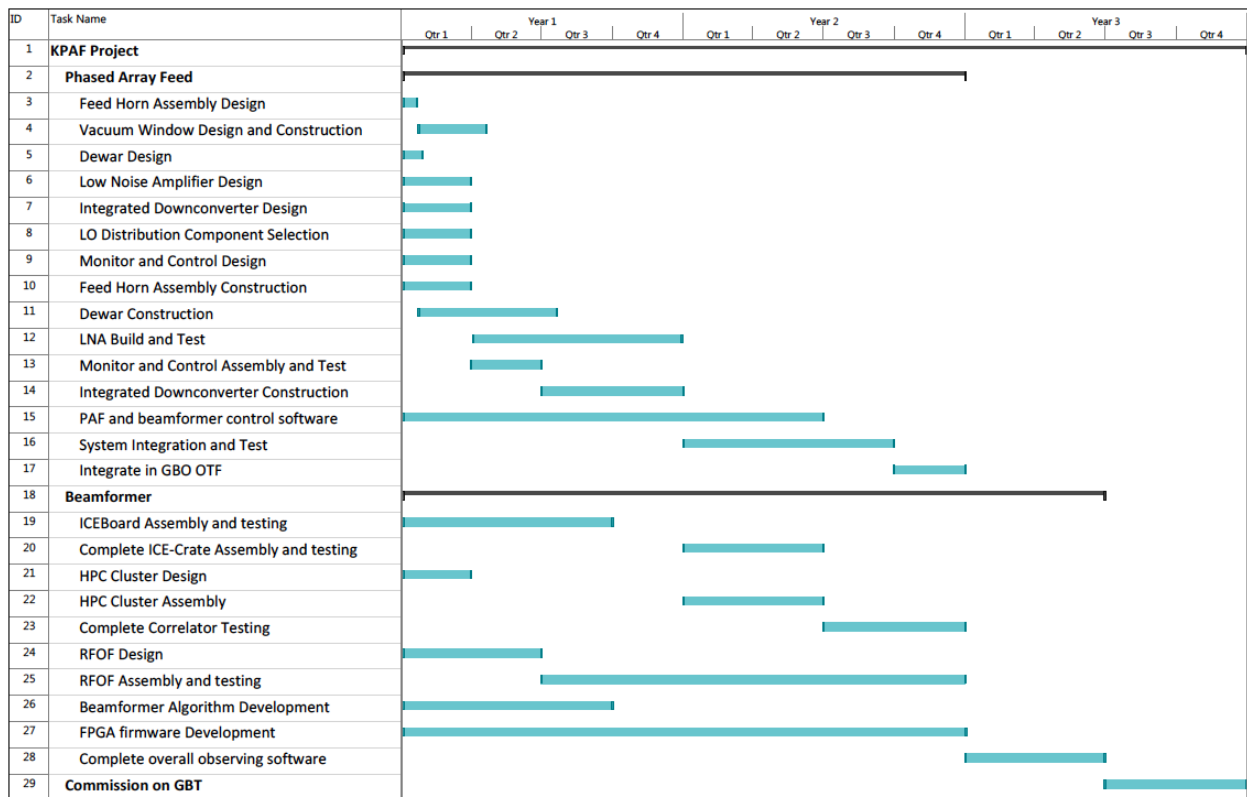


Figure 5: Project Timeline

⁵<https://sites.nationalacademies.org/DEPS/astro2020/index.htm>

4 Broader Impacts

4.1 Education

Through multiple joint projects and educational activities West Virginia University and Green Bank Observatory have developed a comprehensive educational program delivering knowledge to a broad spectrum of students interested in radio astronomy, engineering and computer science. Projects are being developed to reach high school science teachers and students, in addition to undergraduate and graduate students from WVU and elsewhere. While the educational activities within the current submission will be strongly linked to the ongoing and previously developed programs at WVU and GBO, several new activities will be implemented, including the involvement of graduate and undergraduate students in the design and validation of the proposed instrument.

New results and developments will be disseminated through publications in peer-reviewed journals and conference proceedings, while new course material for a graduate level course on Array Design and Signal Processing will be developed. A web page containing all course material will be posted through the Computer Science and Electrical Engineering department at WVU and will be maintained by project personnel.

Once developed, lecture notes and exercise problems will be posted online for public consumption and regularly updated. In addition to a new graduate level course, we intend to add illustrative labs to the existing courses ‘Signal and Systems I and II’, two junior level courses presently offered at WVU. The new labs will illustrate the unique features of phased arrays and beam-formers through the involvement of the Fourier transform, and concepts of sampling and modulation as well as other basics of digital signal processing. Illustration of more complex concepts will be done using the ‘GNU radio’ open source software defined radio package.

4.2 Technology Transfer

A large proportion of the proposed instrument’s system components are general purpose, appropriate to a wide variety of applications within radio astronomy and elsewhere. The beam-former hardware, for example is a generic correlator with 256 inputs and 400 MHz of bandwidth. With respect to radio astronomy, this system could be re-tasked for use with any other focal plane array or interferometer. In a broader context, the beam-former could be used for radar receiver signal processing. As future instrumentation projects at the GBT include both beam-forming arrays at high frequencies (above K-band) and a planetary radar system, the beam-former proposed here would provide immediate and obvious benefits to the knowledge base at the GBO.

The correlator described above is high-speed and relatively inexpensive, this has the potential to be a key enabling technology in the field of wireless communications. The experience, components and overall approach developed for the proposed PAF are likely to be directly applicable to ‘massive MIMO’ where hundreds or thousands of antennas are used to increase the number of signal paths for improved link reliability and/or data rate (Rusek et al., 2013).

References

- Bandura, K., Addison, G. E., Amiri, M., et al. 2014, *Ground-based and Airborne Telescopes V*, 914522
- Bandura, K., Cliche, J. F., Dobbs, M. A., et al. 2016, *Journal of Astronomical Instrumentation*, 5, 1641004
- Bandura, K., Bender, A. N., Cliche, J. F., et al. 2016, *Journal of Astronomical Instrumentation*, 5, 1641005
- Bietenholz, M. F., Kamble, A., Margutti, R., et al. 2018, *MNRAS*, 475, 1756
- Braatz, J., Pesce, D., Condon, J., et al. 2019, *BAAS*51, 446
- Butterfield, N., Barnes, A., Sormani, M., et al. 2019, *BAAS*51, 460
- Friesen, R. K., Pineda, J. E., co-PIs, et al. 2017, *ApJ*, 843, 63
- Hacar, A., Tafalla, M., & Alves, J. 2017, *A&A*, 606, A123
- Hacar, A., Tafalla, M., Kauffmann, J., et al. 2013, *A&A*, 554, A55
- Hogge, T., Jackson, J., Stephens, I., et al. 2018, *ApJS*, 237, 27
- Kutkin, A. M., Pashchenko, I. N., Lisakov, M. M., et al. 2018, *MNRAS*, 475, 4994
- Leroy, A. K., Schinnerer, E., Hughes, A., et al. 2017, *ApJ*, 846, 71
- Leroy, A. K., Bolatto, A., Kepley, A., et al. 2018, *Science with a Next Generation Very Large Array*, 483
- Leroy, A. K., Bolatto, A., Rosolowsky, E., et al. 2018, *Science with a Next Generation Very Large Array*, 499
- Leroy, A. K., Bolatto, A. D., Ostriker, E. C., et al. 2018, *ApJ*, 869, 126
- Leroy, A., Bolatto, A. D., Davis, T. A., et al. 2019, *BAAS*51, 373
- Margot, J.-L., Campbell, D., Padovan, S., et al. 2019, *BAAS*51, 120
- McGuire, B. 2019, *BAAS*51, 233
- McGuire, B. 2019, *BAAS*51, 234
- Mena, J., Bandura, K., Cliche, J.-F., et al. 2013, *Journal of Instrumentation*, 8, T10003
- Friesen, R. 2019, *BAAS*51, 441
- Monsch, K., Pineda, J. E., Liu, H. B., et al. 2018, *ApJ*, 861, 77
- Pilipenko, S. V., Kovalev, Y. Y., Andrianov, A. S., et al. 2018, *MNRAS*, 474, 3523

Remijan, A. 2019, BAAS51, 428

Rosero, V., Hofner, P., Kurtz, S., et al. 2019, arXiv e-prints, arXiv:1905.12089

Rosero, V., Hofner, P., Claussen, M., et al. 2016, ApJS, 227, 25

Rusek, F., Persson, D., Lau, B., et al. 2013, IEEE Signal Processing Magazine, 30, 40

Seo, Y. M., Majumdar, L., Goldsmith, P. F., et al. 2019, ApJ, 871, 134

Sokolov, V., Wang, K., Pineda, J. E., et al. 2018, A&A, 611, L3

Thilker, D., Lee, J., Capak, P., et al. 2019, BAAS51, 525

Walsh, A. J., Breen, S. L., Britton, T., et al. 2011, MNRAS, 416, 1764

Williams, G. M., Peretto, N., Avison, A., et al. 2018, A&A, 613, A11

Zhao, W., Braatz, J. A., Condon, J. J., et al. 2018, ApJ, 854, 124